One-photon ionization spectroscopy of jet-cooled oxazole and thiazole: the role of oxygen and sulfur in the π-conjugation of heterocyclic compounds

Songhee Han,[a] Tae Yeon Kang,[a] Sunyoung Choi,[a] Kyo-Won Choi,[a] Sun Jong Baek,[a] Sungyul Lee[b] and Sang Kyu Kim*[a]

Received 2nd January 2008, Accepted 1st April 2008
First published as an Advance Article on the web 16th May 2008
DOI: 10.1039/b719956b

One-photon mass-analyzed threshold ionization (MATI) spectroscopy of jet-cooled oxazole and thiazole has been carried out to give the precise adiabatic ionization energies of 9.5959 ± 0.0006 and 9.3633 ± 0.0009 eV, respectively. The structural change upon ionization has been revealed in the vibrationally resolved one-photon MATI spectra. Simulations based on the Franck–Condon analysis using the molecular structures calculated by the density functional theory reproduce the experiment very well for both molecules. The ionization-driven structural change of thiazole is quite different from that of oxazole in terms of the detailed geometrical shape, ascribed to the difference in the π-conjugation nature of two molecules. The role of oxygen and sulfur in the stabilization of heterocyclic systems is discussed through the inspection of the calculated molecular orbitals involved in the photoionization.

1. Introduction

Photoionization spectroscopy provides the ionization energy and vibrational structures of the cation. The ionization energy, according to Koopmans' theorem, represents the stablization energy of the corresponding molecular orbital while the associated vibrational structure results from the structural change of the molecule upon ionization, giving information about the role of one-electron deficient orbital in the nuclear layout of the molecule. In this regard, the photoelectron spectroscopy has long been widely used for the estimation of molecular orbital energies and associated vibrational features for a number of molecular systems. Obviously, there have been enormous efforts to improve the energy resolution of the photoionization spectroscopy for the last decade. The best energy resolution (<1 cm^{-1}) up to date can now be attained through the zero kinetic energy (ZEKE) or mass-analyzed threshold ionization (MATI) technique in which the supersonic jet and high resolution laser are used in combination for the excitation of the long-lived high *n*-Rydberg states of the molecule prior to the pulsed-field ionization. Especially, one-photon ZEKE/MATI using the vacuum-UV (VUV) laser source is quite useful for the elucidation of the molecular structure–orbital relation since the structural change of the molecule from the neutral state to cation is directly reflected in the one-photon ZEKE/MATI spectrum. Accordingly, the spectral simulation using the Franck–Condon analysis, based on *ab initio* molecular structures, has been so powerful in the interpretation of VUV-MATI spectra for a number of molecular systems such as DNA/RNA bases,[1–4] sulfur compounds,[5] organometallics,[6] and clusters.[7]

Here, we have investigated the photoionization of oxazole and thiazole using VUV-MATI spectroscopy combined with theoretical simulation with the aid of density functional theory (DFT). These particular unsaturated five-membered heterocyclic compounds have been widely used as building blocks of various polymers,[8,9] useful ligands in supramolecular chemistry,[10,11] and also found in many biomolecular systems.[12] Naturally, the physical properties of oxazole and thiazole have been intensively studied for understanding the role of these molecules in many different circumstances at the atomic level. In this work, we have investigated the ionization behavior of two molecules. Both oxazole and thiazole adopt a planar geometry due to the strong π-conjugation,[13–16] consistent with Hückel's $(4n + 2)$ rule for the aromaticity. Meanwhile, because of the intrinsically different nature of oxygen and sulfur atoms, the molecular structure and extent of the π-conjugation of oxazole and thiazole are actually expected to be quite different. This different nature of oxygen and sulfur in the π-conjugation is revealed as the difference in the structural change that oxazole and thiazole undergo upon ionization.

2. Experimental

Oxazole (Aldrich, 98%) and thiazole (Aldrich, 99%) were used without further purification. These were seeded in the Ar carrier gas and expanded into the vacuum chamber through a nozzle orifice (general valve, 0.5 mm diameter) with a backing pressure of 7.60×10^2–1.14×10^3 Torr. The molecular beam chamber equipped with two turbo pumps were evacuated to maintain a background pressure of 10^{-8} Torr. The supersonic jet was collimated through a 1 mm diameter skimmer (Precision) prior to being overlapped with the excitation laser pulse. The vacuum-

[a] *Department of Chemistry and School of Molecular Sciences (BK21), KAIST, Daejeon, (301-750), Republic of Korea. E-mail: sangkyukim@kaist.ac.kr; Fax: 82-42-869-2810; Tel: 82-42-869-2883*
[b] *College of Environmental Science and Applied Chemistry (BK21), Kyunghee University, Kyungki-do, 499-701, Republic of Korea*

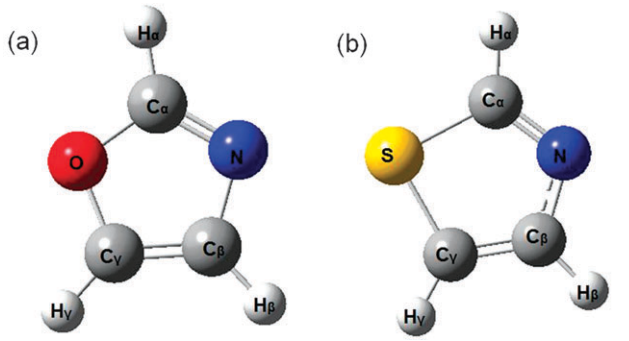

Fig. 1 Optimized geometries of neutral (a) oxazole and (b) thiazole calculated by B3LYP/6-311++G(d,p).

UV (VUV) laser pulse was generated *via* four-wave mixing processes in a Kr gas cell, where the UV laser pulse was fixed at 212.556 or 216.667 nm for the respective Kr $5p[1/2]_0$-$4p^6$ or $5p[5/2]_2$-$4p^6$ transition and tunable VIS laser pulse in the 596–665 nm range were collinearly combined. The VUV pulse was separated from UV and VIS fundamentals using the edge of the collimating CaF_2 lens before it was collinearly overlapped with the molecular beam in a counter-propagating way. The wavelengths of the dye laser outputs were calibrated as those in vacuum using a wavemeter (Coherent; wavemaster).

High-*n*,*l* Rydberg states of molecules which were generated by the VUV laser pulse were pulsed-field ionized ($\sim$10 V cm^{-1}) after the long delay time of 20–30 μs. This delay time was long enough for the separation of the MATI signal from the directly formed ions along the 1 m long time-of-flight tube. Therefore, no spoil field was used for getting MATI spectra. For the accurate measurement of the ionization potential, the MATI spectra were taken as a function of the pulsed field strength (E) and the peak position plotted *vs.* $E^{1/2}$ was extrapolated to get the value at the zero electric field. The generated ions were repelled, accelerated, drifted along the time-of-flight axis, and detected by dual microchannel plates.

Ion signals were digitized by an oscilloscope (LeCroy, LT584M) and stored in a personal computer that controlled all step motors necessary for wavelength scanning.

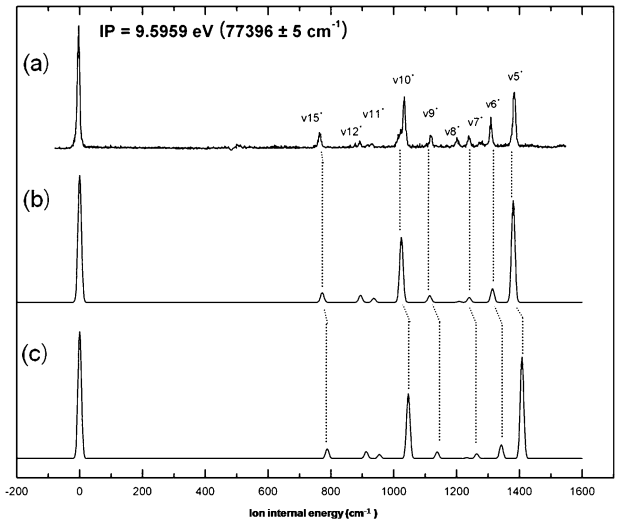

Fig. 2 (a) VUV-MATI spectrum of oxazole with the Franck–Condon simulations using (b) the scaled and (c) unscaled DFT vibrational frequencies (see text). The IP has been accurately determined from the plot of the ionization theshold *vs.* $E^{1/2}$ according to the method described in ref. 6.

Computational details: All calculations were carried out using the Gaussian 03W program package. The minimum energy structures and normal modes for ground neutral and cationic states were calculated using the B3LYP density functional theory (DFT)[17,18] with a basis set of 6-311++G(d,p). The Franck–Condon analysis was performed using the Duschinsky transformation with a code developed by Peluso and coworkers.[19–21]

3. Results and discussion

3.1 Oxazole

The planarity of the cyclic compounds is one of the most critical criteria in the qualitative definition of the π-conju-

Table 1 Calculated geometry parameters of oxazole and thiazole in ground neutral and cationic states by the B3LYP/6-311++G(d, p) method

	Neutral		Cation		Diff[b](%)	
	Oxazole	Thiazole	Oxazole	Thiazole	Oxazole	Thiazole
Summation of internal angles/°	540		540		0	
Dihedral angles/°						
$H_\gamma C_\gamma C_\beta H_\beta$	0		0		0	
$C_\gamma C_\beta N C_\alpha$	0		0		0	
$C_\beta N C_\alpha O(S)$	0		0		0	
$C_\beta N C_\alpha H_\alpha$	180		180		0	
In-plane angle/°						
$\angle H_\gamma C_\gamma C_\beta$	135.34	128.86	133.88	125.94	1.08	2.27
$\angle C_\gamma C_\beta H_\beta$	129.08	124.87	127.61	123.72	1.14	0.92
Bond lengths/Å						
C_γ–O(S)	1.37	1.73	1.32	1.67	+3.77	+3.58
O(S)–C_α	1.36	1.75	1.38	1.82	−1.80	−4.30
C_α–N	1.29	1.30	1.32	1.30	−1.97	−0.44
N–C_β	1.39	1.38	1.34	1.34	+4.15	+2.85
C_β–C_γ	1.36	1.36	1.45	1.45	−6.70	−6.20

[a] Descriptions of geometry parameters based on the index appeared in Fig. 1a and b. [b] Difference between geometry parameters of neutral and cation in each molecule based on the equation of (neutral–cation)/neutral × 100.

Table 2 Ionization potentials (IP) of oxazole

IP/eV	Method	Reference/year
9.5959 ± 0.0006	VUV MATI	This work
9.66	VUV absorption	Ref. 22/2007
10.15	PE(vertical)	Ref. 23/1982
9.9	PE	Ref. 23/1982
9.6	EI	Ref. 24/1976
9.5556	B3LYP/6-311++G(d,p)	This work

gation system. In this aspect, both oxazole and thiazole compounds are known to adopt the planar geometry in the ground electronic states according to other previous and/or present theoretical calculations, Fig. 1 and Table 1. The origin (0^+-0) band at 77 396 cm^{-1} in the VUV-MATI spectrum in Fig. 2 represents the adiabatic ionization energy of oxazole to give the IP value of 9.5959 ± 0.0006 eV, Table 2. This value provides the most precise IP to date, and matches quite well previously reported ones. No low-frequency bands less than 700 cm^{-1} associated with out-of-plane vibrational modes are observed, indicating that the planar geometry of oxazole in the ground state is maintained even after the ionization. Instead, several vibrational bands above ~750 cm^{-1} are found to be strongly excited as the molecule becomes ionized. Band assignments based on DFT (B3LYP) calculations with a 6-311++G(d,p) basis set indicate that those strongly observed MATI bands are all associated with in-plane vibrational modes (Table 3), indicating that oxazole undergoes a severe structural change upon ionization and such a geometrical change is restricted on the molecular plane. Franck–Condon simulation based on theoretical molecular structures from DFT calculations reproduces well the experiment, Fig. 2. Unscaled DFT values are slightly overestimated compared to the experimental frequencies. The application of the scale factor of 0.98 to the DFT vibrational frequencies

Table 3 Vibrational frequencies of oxazole in the neutral and cation ground states

		Neutral	Cation		Descriptions[c]
		IR[a]	DFT[b]	Expt	
A′	ν_1^+		3256.1		CH sym str.
	ν_2^+		3242.8		CH antisym str.
	ν_3^+		3232.6		CH antisym str.
	ν_4^+		1487.9		CH rock.
	ν_5^+		1407.4	1382.5	CH rock.+ OCCN str.
	ν_6^+	1329.8	1341.1	1308.3	CH rock.+ CNC antisym str.
	ν_7^+		1264.5	1238.2	CH rock.
	ν_8^+	1142.5	1232.8	1201.1	Ring breathing
	ν_9^+	1091.1	1137.6	1115.4	CH rock.
	ν_{10}^+	1081.3	1045.4	1033.7	CC str.+CH rock.
	ν_{11}^+	1051.8	954.5	932.5	Ring def.
	ν_{12}^+	899.3	913.0	891.4	Ring def.
	ν_{15}^+	832.0	787.3	763.0	COC str.
A″	ν_{13}^+	909.3	905.7		CH wag
	ν_{14}^+	859.2	877.5		Ring tors.+CH wag.
	ν_{16}^+	749.3	770.9		CH wag.
	ν_{17}^+	646.4	519.2		Ring tors. +CH wag.
	ν_{18}^+		498.3		Ring tors. +CH wag.

[a] Ref. 12. [b] Unscaled; B3LYP/6-311++G(d,p). [c] Description of vibrational modes based on the symbols appeared in Fig. 2(a); def.: deformation, rock.: rocking, str.: stretching, tors.: torsion, wag.: wagging.

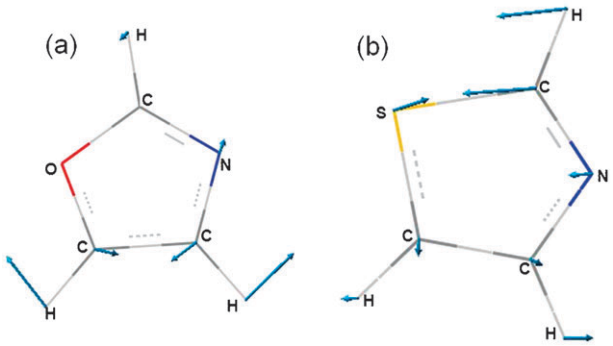

Fig. 3 Vector representations for activated vibrational modes of (a) oxazole (ν_5^+) and (b) thiazole (ν_{16}^+) calculated by DFT (B3LYP/6-311++G(d,p)).

makes the simulated spectrum to be almost perfectly matched with the experiment. This fact demonstrates that the DFT calculation is quite satisfactory in predicting the minimum geometry and vibrational frequencies of the oxazole cation in its ground electronic state. The vector description of the most pronounced normal mode in MATI reflects the geometrical change induced by the ionization (Fig. 3), suggesting that in-plane ring distortion including the H–C–C–H in-plane angle tilt is the main geometrical change of oxazole upon ionization.

It is interesting to point out that the C_β–C_γ bond length is largely increased from 1.36 Å of neutral to 1.45 Å of ion whereas C_α–O and C_α–N bond lengths are moderately increased from 1.36 and 1.29 to 1.38 and 1.32 Å, respectively. Meanwhile, the C_γ–O and C_β–N bond lengths are calculated to be decreased from 1.37 and 1.39 to 1.32 and 1.34 Å, respectively, upon the ionization, Table 1. This geometrical change fully reflects the shape of the molecular orbital from which an electron is removed in the ionization process. As depicted in Fig. 4, the highest-occupied molecular orbital (HOMO) of the neutral oxazole shows the nodal plane crossing C_γ–O and C_β–N bonds. The ionization means the

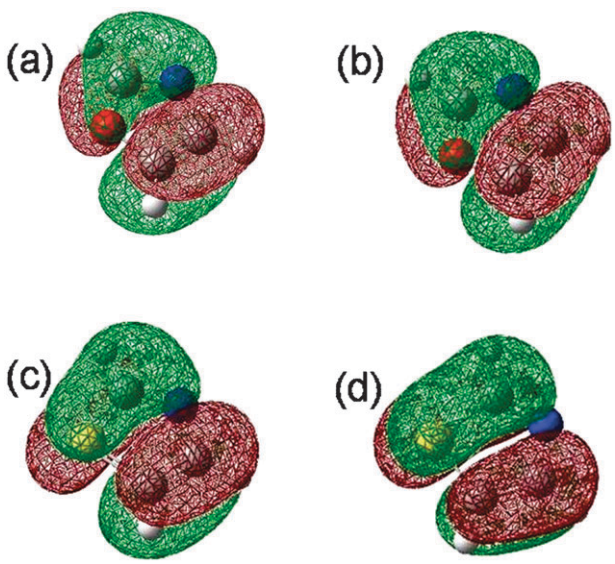

Fig. 4 (a) HOMO and (b) SOMO of oxazole; (c) HOMO and (d) SOMO of thiazole.

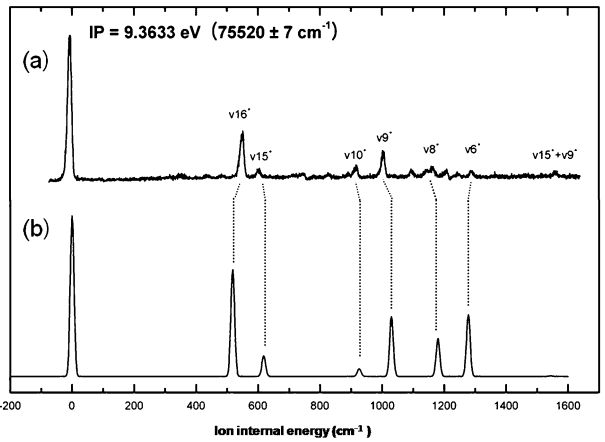

Fig. 5 (a) VUV-MATI spectrum of thiazole and (b) the simulation with unscaled DFT vibrational frequencies.

deficiency of the electron in HOMO, and the π-bonding character along C_β–C_γ, C_α–O and C_α–N is diminished (increasing the bond length) whereas the antibonding character along C_γ–O and C_β–N bonds is decreased (decreasing the bond length) as the molecule is ionized. The qualitative prediction based on the inspection of HOMO is quite consistent with the calculated results in Table 1. The singly-occupied molecular orbital (SOMO) of the oxazole cation is calculated to be quite similar to HOMO of the neutral in terms of the orbital shape governing the overall structure of the molecule, confirming the above interpretation.

3.2 Thiazole

In thiazole, the oxygen atom in oxazole is replaced with sulfur. Since the valence orbital of sulfur is 3p whereas other atoms on the ring have 2p valence orbitals, the π-conjugation is expected to be less stabilized from an energetic point of view. On the other hand, the strong π-conjugation over the entire thiazole ring forces the in-plane nonbonding orbital of sulfur to have the strong sp^2-hybridization so that the HOMO has a character of π-bonding. As expected, the C_α–S and C_γ–S bonds of thiazole are calculated to be much longer than C_α–O and C_γ–O in oxazole, respectively, whereas other bond lengths are more or less the same for the two molecules, Table 1 and Fig. 1. The VUV-MATI spectrum of thiazole shows a strong origin band at 75 520 cm^{-1}, giving an adiabatic ionization potential of 9.3633 ± 0.0009 eV, as shown in Fig. 5. This IP value is around 0.15–0.20 eV less than in the previously reported ones. The DFT (B3LYP/6-311++G(d,p)) value of 9.2932 is very close to the experiment (Table 4).

Table 4 Ionization potentials (IP) of thiazole

IP/eV	Method	Reference/year
9.3633 ± 0.0009	VUV MATI	This year
9.54	PIES[a]	Ref. 25/2006
9.5	EI	Ref. 26/1988
9.50	PE	Ref. 27/1979
9.2932	B3LYP/6-311++G(d,p)	This year

[a] Penning ionization electron spectroscopy.

Table 5 Vibrational frequencies of thiazole in the neutral and cationic ground states

X		Neutral	Cation		Descriptions[c]
		IR[a]	DFT[b]	Expt	
A′	ν_1^+		3225.5		CH sym str.
	ν_2^+		3211.8		CH antisym str.
	ν_3^+		3210.7		CH antisym str.
	ν_4^+		1441.7		CH rock + CNC sym str.
	ν_5^+	1383.7	1322.2		CH rock
	ν_6^+	1325.8	1277.4	1292.4	CNC str. + CH rock.
	ν_7^+	1240.5	1253.4		CH rock.
	ν_8^+	1125.1	1179.0	1165.1	CH rock.
	ν_9^+	1043.6	1030.5	1002.6	CH rock.
	ν_{10}^+	879.3	926.4	916.2	CS str.
	ν_{12}^+		847.8		Ring def.
	ν_{15}^+	797.4	618.3	604.6	Ring def.
	ν_{16}^+	717.6	519.0	550.8	CS str.
	$\nu_{15}^+ + \nu_{10}^+$		1544.7	1559.5	CS str. + ring def.
A″	ν_{11}^+	866.5	887.5		CH wag.
	ν_{13}^+		780.6		CH wag.
	ν_{14}^+		761.7		CH wag.
	ν_{17}^+		493.8		Ring tors. + CH wag.
	ν_{18}^+		346.5		Ring tors. + CH wag.

[a] Ref. 13. [b] Unscaled; B3LYP/6-311++G(d,p). [c] Description of vibrational modes based on the symbols appearing in Fig. 2b; def.: deformation, rock.: rocking, str.: stretching, tors.: torsion, wag.: wagging.

Similarly to the oxazole case, there is no low-frequency bands in the MATI spectrum, confirming that the thiazole also retains planar geometry after being ionized, Fig. 5. The strongly observed MATI band at around 550 cm^{-1} (ν_{16}^+) is ascribed to the mode involving mainly C_α–S stretching motion as depicted in Fig. 3. The Franck–Condon simulation based on DFT molecular structures and vibrational frequencies (Tables 1 and 5) matches the experiment quite well, Fig. 5. The vibrational band intensities of thiazole are relatively poorly reproduced compared to those of oxazole, indicating that the theoretical prediction for the thiazole ionization is less accurate compared to that for oxazole at the present level of our DFT calculations. It is also noteworthy that a single scale factor cannot be applied to all calculated vibrational modes to match the experiment for thiazole, contrary to the case of oxazole. However, despite the less perfect match with the experiment, the simulation confirms that the structural change of thiazole upon ionization is quite drastic in terms of the C_α–S and C_β–C_γ bond lengths, as calculated and listed in Table 1.

The increase ratio of the C_α–S bond length for thiazole is much larger than that of C_α–O for oxazole whereas the decrease ratios of C_γ–S and C_γ–O bond lengths upon ionization are more or less the same for both molecules. This difference in the ionization-driven structural changes of the two molecules, as being reflected in different MATI spectra, is attributed to the difference of the detailed shape of the molecular orbitals of oxazole and thiazole. As shown in Fig. 4, the nodal plane of HOMO of neutral thiazole crosses the C_γ–S bond and near the center of nitrogen atom whereas that of oxazole crosses C_γ–O and C_β–N bonds (*vide supra*). The different nature of the molecular orbitals of oxazole and thiazole is found to be more evident for SOMO. Namely, the nodal plane of SOMO of the thiazole cation bisects the C_γ–S

bond and nitrogen atom whereas that of oxazole bisects the C_γ–O and C_β–N bonds, Fig. 4. Therefore, the π-bonding of thiazole is more localized on the C_γ–S bond, giving the larger increase of the bond length upon the depletion of the electron compared to the case of oxazole. It is quite intriguing that such a detailed shape of molecular orbital results in the big difference in the geometrical change of two molecules when it is driven by the ionization. Naturally, the different molecular orbital shape comes from the intrinsic difference of the atomic orbitals of sulfur and oxygen and their role in the π-conjugation of heterocyclic compounds. The larger distance of C–S than C–O, which is probably due to the size difference of the respective 3p (S) and 2p (O) orbitals in the zeroth order picture, should be responsible for such a subtle difference in the orbital shapes of the two heterocyclic molecules.

4. Conclusion

In summary, we report here the most accurate and precise ionization potentials of oxazole and thiazole to date, which are superior to previously measured ones. Franck–Condon analysis based on DFT calculations of molecular structures and vibrational frequencies makes possible the stringent test of theoretical calculations compared to the experiment. The extent of aromaticity in the heterocyclic compound has often been described quite qualitatively in organic or biological chemistry for the explanation of associated chemical reactivity in various chemical environments. Here, we have thoroughly examined the nature of HOMO and SOMO for oxazole and thiazole through the vibration-resolved VUV-MATI spectroscopy, giving a quantitative description of the electron role in the molecular structure and its change upon ionization. Sulfur is ubiquitous in chemistry and biology, and our effort for the quantitative analysis of the associated property of sulfur compounds will be quite helpful for understanding sulfur chemistry at the atomic level.

Acknowledgements

This work was supported by Korea Research Foundation (KRF-2006-311-C00078), KOSEF (R01-2007-000-10766-0), SRC (R11-2007-012-01002-0), and KISTI supercomputing centre (KSC-2007-S00-1027).

References

1. K.-W. Choi, D.-Sik. Ahn, J.-H. Lee and S. K. Kim, *J. Phys. Chem. A*, 2006, **110**(8), 2634.
2. K.-W. Choi, J.-H. Lee and S. K. Kim, *Chem. Commun*., 2006, **78**, 1.
3. K.-W. Choi, J.-H. Lee and S. K. Kim, *J. Am. Chem. Soc*., 2005, **127**, 15674.
4. K.-W. Choi, D.-S. Ahn, S. Lee, H. Choi, K.-K. Baeck, S.-U. Heo, S. J. Baek, Y. S. Choi and S. K. Kim, *ChemPhysChem*, 2004, **5**, 737–739.
5. S. Choi, K.-W. Choi, S. K. Kim, S. Y. Chung and S. Lee, *J. Phys. Chem. A*, 2006, **110**, 13183.
6. K.-W. Choi, S. Choi, S. J. Baek and S. K. Kim, *J. Chem. Phys*., 2007, **126**, 034308.
7. K.-W. Choi, D.-S. Ahn, S. Lee and S. K. Kim, *J. Phys. Chem. A*, 2004, **108**, 11292–11295.
8. J. Tang, L. Jiang, W. Sun and Z. Shen, *React. Funct. Polym*., 2004, **61**, 405–410.
9. T. Yamamoto, K. Namekawa, I. Yamaguchi and T.-A. Koizumi, *Polymer*, 2007, **48**, 2331–2337.
10. T. Riis-Johannessen, J. C. Jeffery, A. P. H. Robson, C. R. Rice and L. P. Harding, *Inorg. Chim. Acta*, 2005, **358**, 2781–2798.
11. M. Poyatos, A. Maisse-Francois, S. Bellemin-Laponnaz and L. H. Gade, *Organometallics*, 2006, **25**, 2634–2641.
12. O. Ya. Shatursky, T. M. Volkova, O. V. Romanenko, N. H. Himmelreich and E. V. Grishn, *Biochim. Biophys. Acta*, 2007, **1768**, 207–217.
13. M. Muniz-Miranda, *Vib. Spectrosc*., 1999, **19**, 227–232.
14. D. LeGourrierec, V. A. Kharlanov, R. G. Brown and W. Rettig, *J. Photochem. Photobiol., A*, 2000, **130**, 101–111.
15. J. R. Davidson, A. K. Burnham, B. Siegel, P. Beak and W. H. Flygare, *J. Am. Chem. Soc*., 1974, **96:24**.
16. I. D. L. Albert, T. J. Marks and M. A. Ratner, *J. Am. Chem. Soc*., 1997, **119**, 6575–6582.
17. A. D. Becke, *J. Chem. Phys*., 1993, **98**, 5648.
18. C. Lee, W. Yang and R. G. Parr, *Phys. Rev. B*, 1988, **37**, 785.
19. F. Duschinsky, *Acta Physicochim. URSS*, 1937, **7**, 551.
20. A. Peluso, F. Santoro and G. D. Re, *Int. J. Quantum Chem*., 1997, **63**, 233.
21. R. Borrelli and A. Peluso, *J. Chem. Phys*., 2003, **119**, 8437.
22. M. H. Palmer, G. Ganzenmuller and I. C. Walker, *Chem. Phys*., 2007, **334**, 154–166.
23. T. Kobayashi, T. Kubota, K. Ezumi and C. Utsunomiya, *Bull. Chem. Soc. Jpn*., 1982, **55**, 3915.
24. H.-E. Audier, M. Fetizon, Y. Henry and T. Prange, *Org. Mass Spectrom*., 1976, **11**, 1047.
25. M. Yamazaki, N. Kishimoto and K. Ohno, *J. Phys. Chem. A*, 2006, **110**, 7097–7104.
26. H. Daamen, A. Oskam, D. J. Stufkens and H. W. Waaijers, *Inorg. Chim. Acta*, 1979, **34**, 253.
27. C. S. Ra, S. C. Kim and G. Park, *THEOCHEM*, 2004, 173–178.